

Analysis of Superconducting Microstrip Lines and Resonators Using the Complex Resistive Boundary Conditions and the Variational Principle

Robert C. Qiu and I-Tai Lu

Abstract—A full wave characterization of high-temperature superconducting (HTS) microstrip lines and resonators is formulated based on the complex resistive boundary conditions (CRBC) of HTS. A variational approach is used to extend the applicable parameter range of the CRBC.

I. INTRODUCTION

HTS devices have recently become increasingly important as a result of their desirable merits such as wide bandwidth, low noise, and good power efficiency. However, the properties of HTS films are unlike those of normal metals and cannot be properly modeled by existing computer aided design (CAD) packages [1]. The need to incorporate full wave methods for analyzing HTS devices into the existing CAD codes is acute. One advantageous approach that satisfies this need is the CRBC [2]. Using the CRBC method to represent superconducting strips as zero-thickness complex resistance sheets, the HTS can then be modeled by almost any existing approaches that can be used for conventional microstrips.

The theoretical basis of CRBC is that the HTS effect can be accounted for by an infinitesimally thin current sheet when the thickness of the strip is smaller than the effective penetration depth. In the conventional CRBC method, the current sheet is placed directly on the dielectric slab. This approximation implies the current concentration is on the interface between the dielectric substrate and the superconductor strip; however, this is not true. The effective current sheet should be located somewhere within the superconductor strip. In fact, the two results obtained by placing the current sheet at the top and bottom boundaries represent approximately the upper and lower bounds, respectively, of the true solution. Therefore, an appropriate “variational average” from these two reference results can be more accurate than the conventional one. This argument is based on the TEM approximation of the fundamental mode where the variational approach [3] for transmission lines can be directly applied. Thus, the applicable parameter (strip thickness) range of the CRBC can be extended by incorporating the variational principle.

For a thicker superconductor strip, the current distribution may spread out and does not concentrate at an infinitesimally thin sheet. But the CRBC model with the above mentioned variational approach remains useful to a certain extent for numerical computation as long as the two reference results still represent approximately the two bounds of the true solution. This essential feature is very important for practical engineering applications because the existing CAD codes for metal strips, patches, etc. can now be extended easily to include superconductor films.

II. FORMULATION

Based on the London equations and the two-fluid model [2], the complex conductivity σ_s for a superconductor strip is given as $\sigma_s = \sigma_n(T/T_c)^4 - j/\omega\mu_0\lambda_L^2(T)$ where σ_n is the normal state

conductivity, T the temperature, T_c the critical temperature, and λ_L the London penetration depth: $\lambda_L^2(T) = \lambda_L^2(0)[1 - (T/T_c)^4]$. If thickness “ t ” is small compared with the $\lambda_L(T)$, the HTS strip can be treated as a zero thickness sheet with the surface impedance $Z_s = \frac{1}{\sigma_s}$ (using the CRBC approach [2]). Based on the spectral domain impedance approach [4], the Fourier transformed electrical fields E and current J have the relationship

$$\begin{bmatrix} E_z \\ E_x \end{bmatrix} = \begin{bmatrix} Z_{11} & Z_{12} \\ Z_{21} & Z_{22} \end{bmatrix} \begin{bmatrix} J_z \\ J_x \end{bmatrix} \quad (1)$$

if the superconductor strip is treated as a normal conductor. Here, Z_{ij} , $i, j = 1, 2$ are the Fourier transforms of the Green dyadics. Considering the superconducting effects, we need simply to modify (1) by replacing the diagonal elements Z_{ii} , $i = 1, 2$ by $Z_{ii} - Z_s$. Then, the propagation constant $v = \alpha + j\beta$ can be obtained by solving (1) if the position of the current sheet is specified.

Let β_1 and β_2 be the phase constants obtained by solving (1) when the current sheet is placed at two reference planes (e.g., the top and the bottom interfaces of HTS strip). From the variational principle (see the derivation in Appendix), the true phase constant is $\beta = (\beta_1\beta_2)^{1/2}$. Following the basic transmission line theory, the modal impedance Z_0 is defined here as P/I_0^2 where P is the time-average Poynting power, and I_0 is the effective current flow along the strip. The unloaded quality factor Q_0 for a $\lambda/2$ microstrip resonator here is defined as $Q_0 = 2\pi/(1 - e^{-4\pi\alpha/\beta})$ where α and β are, respectively, the attenuation and phase constants at the resonance frequency.

III. RESULTS AND ANALYSIS

Consider, for example, the top superconductor strip of the microstrip line in Fig. 1. Shown in Fig. 2(a) is the dependence of the normalized phase velocity $\omega/(\beta v)$ on the thin-film strip thickness “ t .” Here, the medium velocity is $v = (\mu_0\epsilon)^{-1/2}$. The two reference planes are chosen to be the center and the bottom of the HTS strip. We choose the width w to be much larger than the substrate thickness “ s ” so that results obtained using the variation approach can be compared with the analytic solution, which is only valid when $w \gg s$ [5]. Note that our approach is not subject to this restriction. In this simulation, we also set $t = s$, which has been chosen in [2]. Without using the variational approach, it has been shown in Fig. 3 of [2] that the CRBC is accurate only when $t < 10^{-7}$ m (assuming $\lambda_L(0) = 1000$ Å). However, our present results extend the range to 10^{-6} m (an order higher), which is commonly used in practical structures [6]. The error shown near $t = 10^{-6}$ m in Fig. 2(a) can be reduced by choosing the top interface to replace the center plane as one of the two reference planes because the equivalent current sheet is located closer to the center of the HTS strip for larger t . But, in this case, the error of the variational approach at smaller t will slightly increase. Thus, different reference planes can be selected for different thicknesses to obtain optimum accuracy. Fig. 2(b) shows that the characteristic impedance Z_0 agrees well with the analytic solution of the triplet model [5]. Similarly, better agreement for larger t can be obtained using the top and bottom interfaces as the two reference planes.

The effects of the temperature T and the substrate loss $\tan \delta$ on the unloaded quality factor Q_0 of a half wavelength superconductor microstrip resonator (see Fig. 2 of [6]) are shown in Fig. 3(a) and 3(b), respectively. In our numerical simulation (using the parameters in [6]), Q_0 remains almost constant when the temperature is lower than the critical temperature T_c and decreases drastically around

Manuscript received February 23, 1994; revised November 10, 1994.

The authors are with the Department of Electrical Engineering, Weber Research Institute, Polytechnic University, Farmingdale, NY 11735 USA.
IEEE Log Number 9410699.

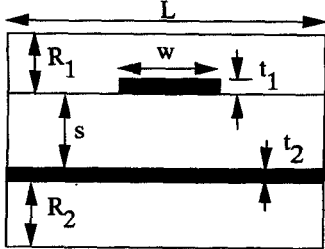


Fig. 1. Geometric configuration.

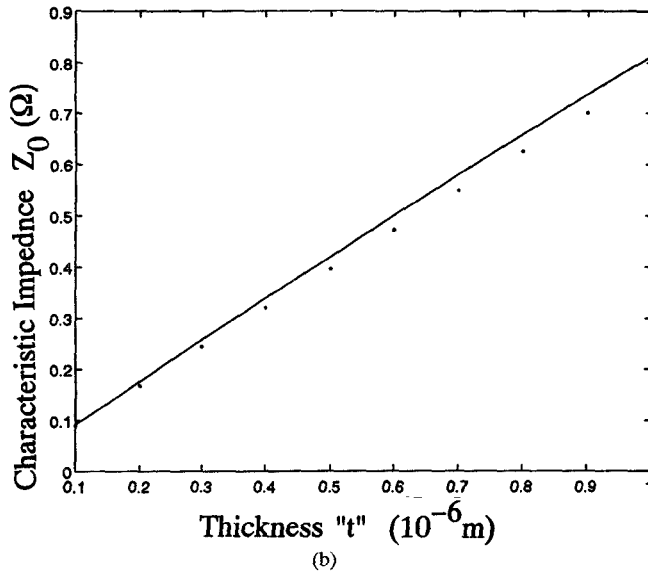
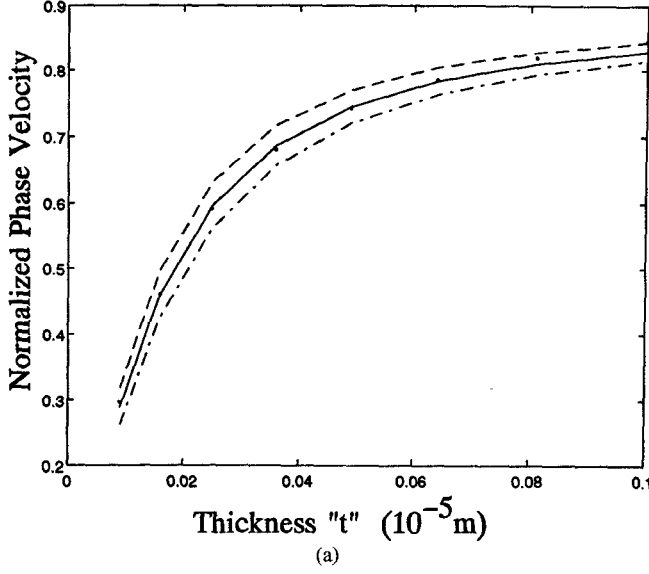
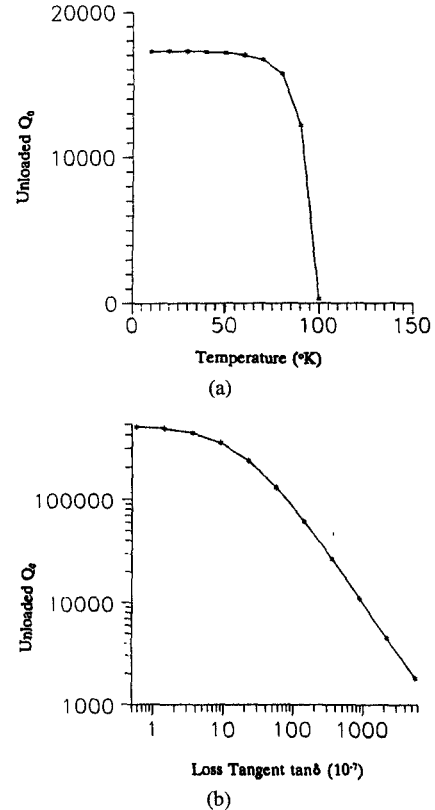


Fig. 2. The dependence of the normalized phase velocity and the characteristic impedance Z_0 on the thin film thickness t of the superconductor microstrip. The analytic solution is represented by the solid line. The variational result is denoted by dots. In Fig. 2(a), dashed and chain-dashed curves represent the results obtained by placing the effective current sheet on the center and the bottom, respectively, of the superconductor strip. Parameters: $f = 10$ GHz, $w = 10^{-3}$ m, $\lambda_L(0) = 0.16 \times 10^{-6}$ m, $\epsilon_r = 24.5$, $\tan \delta = 5.8 \times 10^{-5}$, $L/w = 50$, $\sigma_n = 2.0 \times 10^5$ s/m, $T = 70$ K, $T_c = 91$ K, $R_1 = R_2 = 100w$, $s = t$, $t_1 = t_2 = t$, $c_0 = 3.0 \times 10^8$ m/s.

T_c . This phenomenon is expected theoretically and is also observed in the experiment (see Fig. 4 of [6]). We also observe that Q_0 decreases dramatically when $\tan \delta > 10^{-5}$. Since the loss tangent of practical dielectric materials is of this order, the quality factor of this

Fig. 3. The dependence of the unloaded quality factor Q_0 on the temperature T and the substrate loss $\tan \delta$.

superconductor resonator is dominated by the dielectric loss rather than the superconductor loss. This feature has also been noted in [6].

IV. CONCLUSION

The variational approach is used to improve the numerical accuracy and to extend the applicable parameter (strip thickness) range of the CRBC. The normalized phase velocity, the characteristic impedance of the microstrip line, and the unloaded quality factor of the microstrip resonator are numerically simulated. Our results are compared with the analytic solution of a parallel plate waveguide and the experimental results of a microstrip resonator. With the variational approach, the CRBC approach now can be employed to analyze HTS thin films with practical thicknesses.

APPENDIX

Since the fundamental mode can be approximated as a TEM mode, its phase constant β can be approximated by $(C/C_0)^{1/2}k_0$ where C_0 and C are, respectively, the capacitance per length for the microstrip line without and with the dielectric present and $k_0 = \omega(\mu_0 \epsilon_0)^{1/2}$. Accordingly, the two bounds of β are $\beta_u = (C_u/C_{0u})^{1/2}k_0$, $u = 1, 2$. The subscript "1" or "2" denotes, respectively, that the complex surface impedance Z_s is placed at a certain plane of the superconductor strip. Generally speaking, C_0 and C are unknown because the true location of the impedance sheet is unknown. But we can easily find values $C_1(C_{01})$ and $C_2(C_{02})$ as the two bounds of $C(C_0)$, i.e., $C_1 \leq C \leq C_2$ and $C_{01} \leq C_0 \leq C_{02}$. Based on the variational principle [3], various averages can be adopted to estimate the true capacitances $C(C_0)$. Here, we use the geometric average, $C = (C_1 C_2)^{1/2}$ and $C_0 = (C_{01} C_{02})^{1/2}$. This implies that the true β can also be approximated by the geometric average of β_1 and β_2 , i.e., $(\beta_1 \beta_2)^{1/2}$.

REFERENCES

- [1] R. B. Hammond, G. L. Hey-shipton, and G. L. Matthaei, "Designing with superconductors," *IEEE Spectrum*, pp. 34-39, Apr. 1993.
- [2] D. Nghiem, J. T. Williams, and D. R. Jackson, "A general analysis of propagation along multi-layer superconducting stripline and strip transmission lines," *IEEE Trans. Microwave Theory Tech.*, vol. 39, no. 9, pp. 1553-1565, Sept. 1991.
- [3] W. Lin, "A critical study of the coaxial transmission line utilizing conductors of both circular and square cross sections," *IEEE Trans. Microwave Theory Tech.*, vol. 30, no. 11, pp. 1981-1988, 1982.
- [4] T. Itoh, "Spectral domain imittance approach for dispersion characteristics of generalized printed transmission lines," *IEEE Trans. Microwave Theory Tech.*, vol. MTT-28, no. 7, pp. 733-736, July 1980.
- [5] J. C. Swihart, "Field solution for a thin-film superconducting strip transmission line," *J. Appl. Phys.*, vol. 32, no. 3, Mar. 1961, pp. 461-469.
- [6] C. Wilker *et al.*, "5 GHz High-temperature-superconductor resonators with high Q and low power dependence up to 90 K," *IEEE Trans. Microwave Theory Tech.*, vol. 39, no. 9, pp. 1462-1467, Sept. 1991.

Characterization of Off-Slot Discontinuity in Unilateral Fin Line

Alok Kumar Gupta and Animesh Biswas

Abstract—A new type of fin line discontinuity, which consists of a rectangular conducting strip placed transversely on the back side of the air dielectric interface containing the slot, is characterized in this work. Modeling of the fin line cavity containing the discontinuity is carried out using hybrid mode analysis, and then the Transverse Resonance Technique is used to extract equivalent circuit parameters of the discontinuity. Suitable sets of basis functions are chosen for accurately representing the field in the slot and the current on the strip. Calculated results are compared with the measured results for a sample discontinuity to validate the choice of the basis functions.

I. INTRODUCTION

The off-slot discontinuity (discontinuity being in a plane which does not contain a slot) presented in this paper is useful in the realization of filter circuits. This type of discontinuity can also be used for providing dc bias to the active devices mounted across the slot. This paper presents an analysis of the off-slot discontinuity using the Transverse Resonance Technique proposed by Sorrentino and Itoh [1]. This technique involves application of the transverse resonance condition to a model of a fin line cavity containing the discontinuity. The accuracy of the equivalent circuit parameters of the discontinuity depends directly on the accuracy with which the resonant length of the cavity can be determined. This, in turn, depends on the accuracy of the assumed slot field distributions and strip current distributions. In this paper, besides using a rigorous hybrid mode analysis, suitable basis functions are chosen [2], [3] which account for the fringing fields at the edges. The validity of the assumed basis function is verified by measuring the transmission coefficient of sample discontinuity in the unilateral fin line and comparing it to the theoretical results. The discontinuity is used in realizing a filter by cascading it in the fin line, and the response is found suitable for a low-pass filter application [4].

Manuscript received August 19, 1993; revised November 10, 1994.

The authors are with the Department of Electrical Engineering, Indian Institute of Technology, Kanpur-208016, India.
IEEE Log Number 9410690.

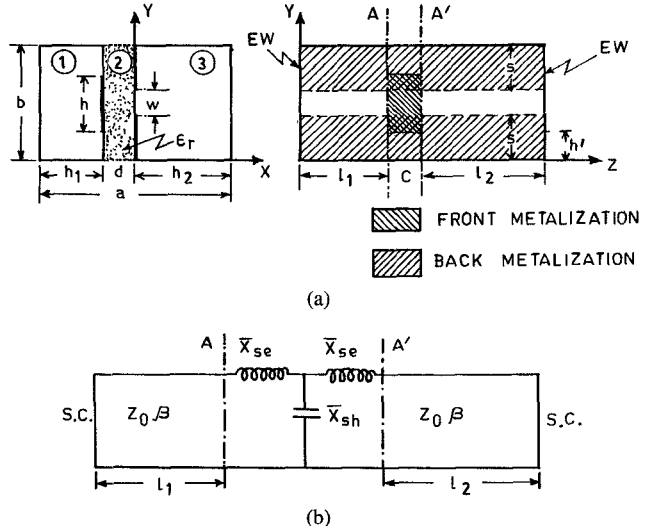


Fig. 1. (a) Cross-sectional and longitudinal views of a unilateral fin line cavity housing the off-slot discontinuity. (b) Equivalent circuit of (a).

II. ANALYSIS

Fig. 1(a) shows the cross-sectional and longitudinal views of a fin line cavity containing the off-slot discontinuity. The equivalent circuit of the fin line cavity with the discontinuity represented as a *T*-equivalent network is shown in Fig. 1(b).

A. Characteristic Equation of the Cavity

First, the fields in the three regions of the cavity [marked 1, 2, and 3 in Fig. 1(a)] are expanded in terms of modal fields with unknown coefficients. Then, by satisfying the boundary conditions followed by the application of orthogonality conditions at various dielectric-air interfaces, we can express all the field coefficients in terms of a transformed electric field at the slot aperture and currents on the conducting strip.

Next, by applying Galerkin's procedure, we get a set of homogeneous equations as

$$\begin{aligned}
 & \sum_{p=0}^P C_{Ep} \sum_{m=1}^{\infty} \sum_{n=0}^{\infty} G_{11} L_{1emn}^{(p)} L_{2emn}^{(i)} \\
 & + \sum_{q=0}^Q D_{Eq} \sum_{m=1}^{\infty} \sum_{n=0}^{\infty} G_{12} L_{2emn}^{(q)} L_{2emn}^{(i)} \\
 & + \sum_{r=0}^R C_{Ir} \sum_{m=1}^{\infty} \sum_{n=0}^{\infty} G_{13} L_{1Imn}^{(r)} L_{2emn}^{(i)} \\
 & + \sum_{s=0}^S D_{Is} \sum_{m=1}^{\infty} \sum_{n=0}^{\infty} G_{14} L_{2Imn}^{(s)} L_{2emn}^{(i)} \\
 & = 0 \quad i = 1, 2, \dots, Q
 \end{aligned} \tag{1a}$$

$$\begin{aligned}
 & \sum_{p=0}^P C_{Ep} \sum_{m=0}^{\infty} \sum_{n=1}^{\infty} G_{21} L_{1emn}^{(p)} L_{1emn}^{(j)} \\
 & + \sum_{q=0}^Q D_{Eq} \sum_{m=0}^{\infty} \sum_{n=1}^{\infty} G_{22} L_{2emn}^{(q)} L_{1emn}^{(j)}
 \end{aligned}$$